Small signal gain and loss measurement of a CW Nd:YAG laser using an antiresonant ring interferometer

Saeed Ghavami Sabouri* **and Alireza Khorsandi**

Department of Physics, University of Isfahan, 81746-73441 Isfahan, I. R. Iran

**Corresponding author: ghavami@sci.ui.ac.ir*

Received November 14, 2011; accepted January 10, 2012; posted online, 2012

An antiresonant ring (ARR) interferometer configuration is introduced for the characterization of a continuous wave (CW) Nd:YAG laser output. The output of the ARR device is precisely characterized to determine the gain and loss of a laboratory CW Nd:YAG laser by using the Findlay-Clay approach. The ARR arm is then experimentally arranged inside the cavity of an arranged high power side-pumped CW Nd:YAG laser. A coated beam splitter with 50–50% reflectivity at normal incidence is placed inside the cavity to provide a wide range of reflectivity from 0 to 100%. This is performed by a rotatable stage and tilting the beam splitter by 10° with the steps of 0.05. By changing the input electrical power of the laser pump the variation of the output laser power is monitored for 20 individual reflectivity of ARR arm. Average pump threshold power of about 180 W is obtained. With the help of the derived equations and obtained threshold power, small signal gain and loss associated with the emerging beam is estimated. It is verified that the former is very dependent to the input parameters. Laser efficiency is also measures 5.6% which is quite comparable with the reported values.

OCIS codes: 140.0140, 120.0120.

doi: 10.3788/COL201210.061405.

Antiresonant ring (ARR) configuration was proposed and analyzed by. Sagnac for the first time[1]. Soon after ARR concepts was applied in pulsening a CO_2 laser by cavity damping[2]. Hereof, pulse shortening of a Nd:YAG laser is also performed with good amplitude stability and short-term reliability[3]. The applications of ARR configuration has been extended to the nonlinear optical properties measurement of thin films. In combination with z-scan technique, measurement of the CdS nonlinear properties was shown to be more sensitive[4]. Most recently ARR arrangement is employed in the experimental setup of a femtosecond optical parametric oscillator (OPO) to obtain a variable output coupling from 1% to about 60%[5]. The output power of a picosecond MgO-PPLN base OPO is optimized by an ARR[6].

Compared with other complicated methods such as degenerate four wave mixing (DFWM)[7], ARR provide very simple and accurate measurement of weak optical nonlinearities. On the other hand, ARR device is very susceptible to the insertion loss provided by the intra cavity elements such as beam splitter (BS). However, a rotatable BS is an essential part of a characteristic ARR to provide a continuous wide range of cavity output coupling.

In this letter, we introduce an ARR configuration for gain and loss calculation of the Nd:YAG laser cavity using Findlay-Clay approach[8]. It is a powerful and easy method to characterize the gain and losses of the laser active material in both continuous wave (CW) and pulsed regime while the laser is operated below or near the threshold[9,10]. When close to threshold, very small perturbation is able to induce serious fluctuations in the power output of the laser. Therefore, the accuracy of the Findlay-Clay approach is strongly depends on the technique used to determine the threshold. In our investigation, derived equations in combination with obtained practical values from the experimentally arranged ARR arm have been used to compute the cavity gain and loss and the efficiency of a CW Nd:YAG laser as well by using the Findlay-Clay plot.

As shown in Fig. 1, an ARR consists of a ring cavity. A BS with a power division ratio close to 50–50%

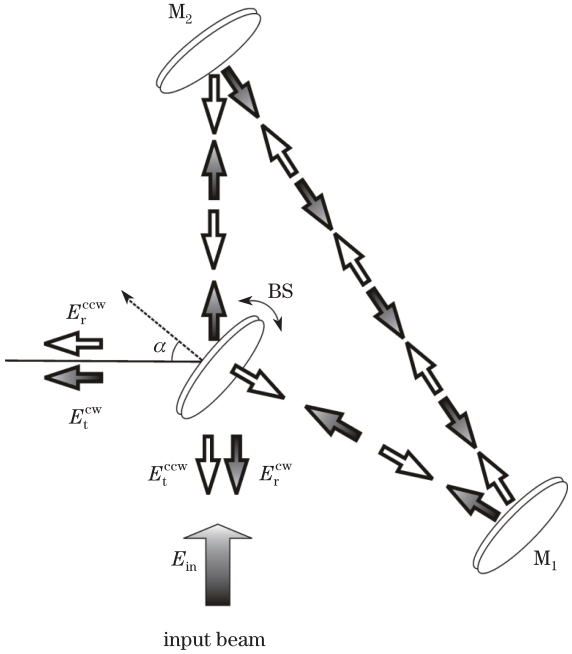

Fig. 1. Optical schematic of the ARR configuration containing a rotatable BS. While the BS is rotated within a certain range of angles symbolized by the reflectivity of the BS can be changed. Mirrors M_1 and M_2 are assumed to have high-reflection (HR) at 45° with respect to the incident laser beam. Black arrows are for clockwise beam, E^{cw} while the white arrows are for counterclockwise beam, E^{ccw}.

divides the input laser beam into two beams traveling in opposite directions possessing phase difference. After a complete round-trip two returning fields will interfere destructively at the BS and transmission reduces to zero. By rotating the BS from the ideal condition, the reflectivity of the ARR can be changed and a portion of the traveling beams will be transmitted. Such variable transmitted intensity can be measured and used to evaluate the important parameters like gain and loss of the laser cavity.

As shown, the electric filed $E_{\rm in}$ associated with the input laser beam is divided into $E^{\rm cw}$ as clockwise and $E^{\rm ccw}$ as counterclockwise waves. After a complete round-trip, a dependence of the reflectivity of the rotatable BS on two variable field amplitudes can be identified as[5]

$$E_{\rm feedback} = E_{\rm t}^{\rm ccw} + E_{\rm r}^{\rm cw} = 2trE_{\rm in}, \quad (1)$$

$$E_{\rm output} = E_{\rm r}^{\rm ccw} + E_{\rm t}^{\rm cw} = (r^2 - t^2)E_{\rm in}, \quad (2)$$

where r and t are the reflectivity and transmission coefficients of the BS, respectively. For a lossless BS, Eq. (1) can be modified to obtain the associated reflectance with the ARR arm as

$$R_{\rm ARR} = \left|\frac{E_{\rm feedback}}{E_{\rm in}}\right|^2 = 4R_{\rm BS}T_{\rm BS}. \quad (3)$$

The same can be done with the Eq. (2) to attain an expression for the transmittance of the ARR geometry as

$$T_{\rm ARR} = \left|\frac{E_{\rm output}}{E_{\rm in}}\right|^2 = |R_{\rm BS} - T_{\rm BS}|^2, \quad (4)$$

where $R_{\rm BS} = r^2$ and $T_{\rm BS} = t^2$ are the reflectance and transmittance of the rotatable BS, respectively.

Therefore by accurate rotating of the BS those $R_{\rm ARR}$ and $T_{\rm ARR}$ of the ARR configuration can be continuously controlled and adjusted to provide a desirable feedback into the cavity. It can be followed by Eq. (3) while the reflectance of the coated BS changes by $R_{\rm BS}$ the reflectance of the ARR changes by twice. If for example by rotation $R_{\rm BS}$ is changed from 50% to 100%, then $R_{\rm ARR}$ will be changed from 100% to 0%. This wide range of ARR reflectivity is very advantageous for optimization of the laser output coupling without consuming time and cost. Starting with Findlay and Clay approach, one can relate pump threshold power $P_{\rm th}$ to the ARR reflectance $R_{\rm ARR}$ associated with the variable BS reflectivity $R_{\rm BS}$ as[8]

$$P_{\rm th} = \frac{AI_{\rm s}}{\eta}\frac{\delta - {\rm Ln}(R_{\rm ARR})}{2}, \quad (5)$$

where A is the cross section area of the laser rod, $I_{\rm s}$ is the confined photon flux in a characterized Nd:YAG crystal which is typically around 2 900 J/cm^2, δ is the cavity loss, and η is the efficiency of the laser. Lasing threshold condition requires the gain to be clamped to the cavity loss that is

$$-{\rm Ln}(R_{\rm ARR}) = 2g_0 l - \delta, \quad (6)$$

where g_0 is the small signal, gain and l is the length of the Nd:YAG crystal. Two last equations can be solved simultaneously to relate pump threshold power $P_{\rm th}$ to the small signal gain g_0 through

$$2g_0 l = \frac{2\eta}{AI_{\rm s}}P_{\rm th}. \quad (7)$$

To evaluate the derived equations, an experimental setup shown in Fig. 2 is provided. The employed Nd:YAG crystal is 64-mm-long cylindrical rod with a diameter of 4 mm. It was operated in side-pumped scheme. Laser pumping was provided by three bars of diode arrays located on the top of a triangle around the Nd:YAG rod.

Output power of the diodes could be changed by variation of the injection current up to 24 A which leads to about 10 W Nd:YAG output power. Those pump diodes and Nd:YAG rod were placed into a silicon jacket. Double ionized pure water was circulated inside the jacket with the capacity of about 6 lit/min to reduce thermal noises superimposed on the output beam. As shown in Fig. 2 the ARR arm was arranged with three high-reflecting mirrors and a rotatable BS. The later was placed on a scaled rotating stage (PR01,Thorlabs Co.) to provide very smooth tilt within the accuracy of 0.05°. It was coated for 50–50 condition at normal incident.

Variation of its reflectivity was measured from about 55% to about 99.99% while the BS was rotated over 10°. This leads to the variation of the ARR reflectivity from about 99.99% to about 0.05%. Those are characterized in Fig. 3.

The BS divides the input Nd:YAG laser beam into two counter-propagating beams having a certain intensity ratio. Returning waves will overlap at the BS and the resultant filed will be emerged from the ARR configuration. Beam profile of such beam is characterized and indicated in Fig. 4.

The difference between vertical and horizontal beam waist can be related to the beam astigmatism occurred in multi-reflections inside the ARR arm.

To evaluate the small signal gain, loss and efficiency of the Nd:YAG laser, pump power threshold measurement is a determinant parameter as shown by Findlay and Clay approach. It can be measured by frequent variation of the input pump power for various injection currents and

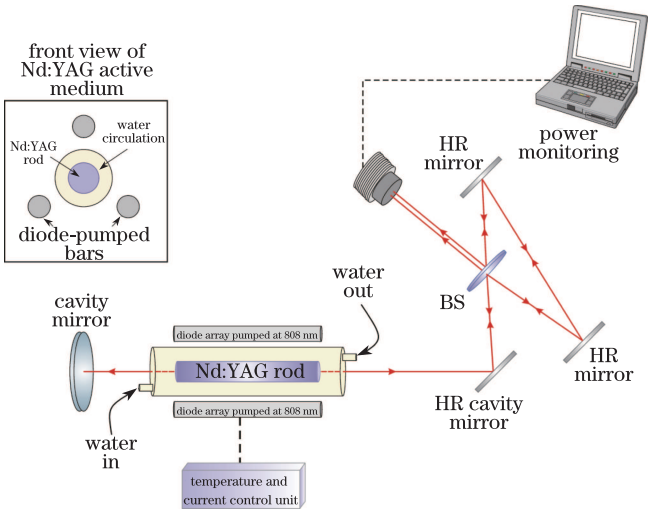

Fig. 2. Schematic diagram of the experimental setup for ARR configuration.

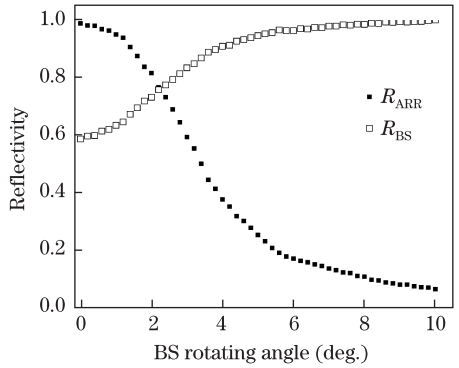

Fig. 3. Variation of the reflectivities R_{BS} and R_{ARR} with rotation angle of BS. It is rotated for 10° with 0.16° ± 0.05° increments.

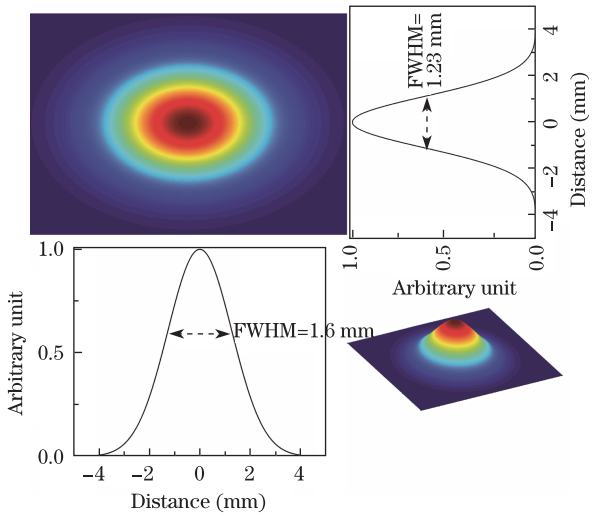

Fig. 4. Characterization of the Nd:YAG beam profile after a complete round-trip inside the ARR optical path.

simultaneous measurement of the laser output power behind the ARR arm while the BS is rotated for a desirable reflectivity. A thermal detector (PM100 & DCMM, Thorlabs Co.) is used to monitor those input and output Nd:YAG laser powers. The results of this measurement are depicted in Fig. 5.

To avoid the complexity, from many curves which could be generated through continuous variation of the BS reflectivity, only those are most distinctive have been appeared in the graph. As could be expected all eight curves are smoothly distributed around a line with different slopes. Indeed they start from a certain point as long as the input power remains low. Thus, by fitting a line into the individual curves the pump threshold powers can be measured by obtaining the values associated with intercept points between the fitted lines and horizontal axis. This gives a range of threshold powers starting from $P_{th} = 157.65$ W for BS reflectivity of $R_{BS} = 0.6$ to $P_{th} = 205.12$ W for BS reflectivity of $R_{BS} = 0.98$.

While the BS inside the ARR arm is rotated to generate a wide range of reflectivity the R_{ARR} can be experimentally measured and the subsequent pump threshold power P_{th} of the laser is immediately determined.

Obtained values provide the possibility of generating another figure which helps to calculate the laser efficiency. Figure 6 shows the relationship between the individual pump threshold power and respective negative logarithmic form of the ARR reflectance.

To calculate the optical characteristics of the laser cavity the required equation can be obtained by simultaneous solution of Eqs. (6) and (7) as

$$-\mathrm{Ln}(R_{ARR}) = \frac{2\eta}{AI_s}P_{th} - \delta. \quad (8)$$

Therefore, the slope of the fitted line in Fig. 6 can be related to the overall efficiency η of the laser. Assuming practical values associated with the employed Nd:YAG laser in our experiment as $A = 12.56$ mm^2, $I_s = 2\,900$ J/cm^2, and the calculated slop as 0.023 W^{-}1, we obtain η=5.6% which is relatively in consistency with the values of Ref. [11]. Moreover, as verified by Eq. (8), loss coefficient can be considered as the longitude of the curve at which the fitted line in Fig. 6 intercepts the vertical axis at P_{th} equal to zero. This gives $\delta = 3.074$ for the utilized Nd:YAG laser cavity.

Once both η and δ are determined, small signal gain of the utilized Nd:YAG laser can be calculated by using Eq. (7) for different operating conditions which can be altered by pump threshold power P_{th}. As indicated in Fig. 7 small signal gain value g_0 is very flexible to the

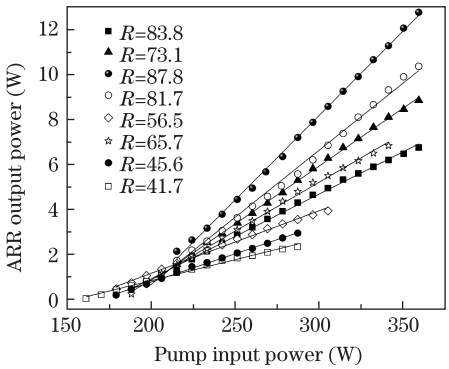

Fig. 5. Variation of the emerged laser power from the ARR arm with the variation of pump input power. The later is changed through frequent variation of injection current of the diode arrays.

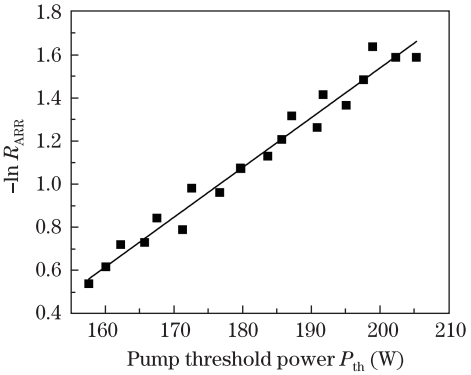

Fig. 6. Pump threshold powers extracted from Fig. 5 versus respective ARR reflectance. The later is shown in a negative logarithmic form as appeared in Eq. (6). Solid line is the linear fit to the experimental data. Slope of the line is 0.023 W^{-1}.

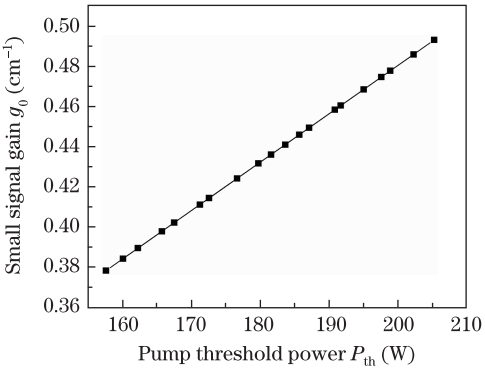

Fig. 7. Calculated small signal gain coefficient for different pump threshold powers. The later can be changed by the plug-in power of the diode pump arrays.

laser operating condition which is induced by different pump threshold powers provided by the input electrical power of the diode arrays.

As clarified in Fig. 7, g_0 is changed in an appropriate range from 0.378 to 0.492 cm^{-1}. Thus under a desirable condition the small signal gain value g_0 can be adjusted for a certain threshold. Therefore Nd:YAG laser operating condition can be optimized for any sets of efficiency, small signal gain and cavity loss as well.

In conclusion the capability of using antiresonant ring interferometer arrangement around the cavity of a Nd:YAG laser is explained and the concepts of such configuration is discussed by derivation of the required equations through Findlay–Clay approach. In the provided ARR experimental setup, the performance of the resultant relations are shown as the calculation of the key laser parameters like small signal gain, cavity loss and laser efficiency as well. The experimental results shows that the fabricated ARR arm around the utilized CW Nd:YAG laser is capable of laser output characterization and optimization. It is further indicated that the small signal gain coefficient is very dependent on the initial operating condition of the laser, which is determined by the input threshold power. Therefore the combination of a input-variable Nd:YAG laser and ARR configuration makes it very suitable for the generation of a particular laser beam and manageable for special applications.

References

1. G. Sagnac, C. R. Acad. Sci. **157,** 1410 (1913).
2. R. Trunta and A. E. Siegman, IEEE J. Quantum Electron. **QE-13,** 955 (1977).
3. G. P. Banfi, G. Gabetta, P. G. Gobbi, and G. C. Reali, Sov. J. Quantum Electron. **20,** 1203 (1990).
4. H. W. H. Lee and R. S. Hughes, Jr., Opt. Lett. **19,** 1708 (1994).
5. A. Esteban-Martin, O. Kokabee, and M. Ebrahim-Zadeh, Opt. Lett. **35,** 16 (2010).
6. S. C. Kumar, A. Esteban-Martin, and M. Ebrahim-Zadeh, Opt. Lett. **36,** 1068 (2011).
7. C. Malouin, A. Villeneuve, G. Vitrant, and R. A. Lessard, Opt. Lett. **21**, 21 (1996).
8. D. Findlay and R. A. Clay, Phys. Lett. **20**, 277 (1966).
9. D. C. Brown, T. M. Bruno, and J. M. Singley, Opt. Express **18,** 16573 (2010).
10. S. Wang, X. Wang, H. Rhee, S. Meister, H. J. Eichler, and J. Chen, Opt. Commun. **283,** 2881 (2010).
11. W. Koechner, *Solid-State Laser Engineering* (Springer, Berlin, 1999).